Cellular/Molecular

Interaction with the Unfolded Protein Response Reveals a Role for Stargazin in Biosynthetic AMPA Receptor Transport

Wim Vandenberghe,[1] Roger A. Nicoll,[1,2] and David S. Bredt[1]
Departments of [1]Physiology and [2]Cellular and Molecular Pharmacology, University of California at San Francisco, San Francisco, California 94143

The transmembrane protein stargazin enhances levels of functional AMPA receptors at the neuronal plasma membrane and at synapses. To clarify the mechanism for this effect, we studied trafficking of the AMPA receptor subunit glutamate receptor 1 (GluR1) in transfected COS7 cells. GluR1 expressed poorly on the surface of these cells and was primarily retained in the endoplasmic reticulum (ER). Stargazin expression strongly increased the surface fraction of GluR1. This effect was not reduced by a dominant-negative dynamin mutant, suggesting that stargazin does not inhibit AMPA receptor endocytosis. Interestingly, upregulation of ER chaperones as part of the unfolded protein response (UPR) both mimicked and occluded the effect of stargazin, suggesting a role for stargazin in ER processing of AMPA receptors. Consistent with this idea, we detected UPR induction in cerebellar granule cells lacking stargazin. Finally, residual AMPA receptor currents in stargazin-deficient neurons were suppressed by inhibition of the UPR. These findings uncover a role for stargazin in AMPA receptor trafficking through the early compartments of the biosynthetic pathway. Furthermore, they provide evidence for modulation of AMPA receptor trafficking by the UPR.

Key words: **glutamate; TARP; trafficking; endoplasmic reticulum; endocytosis; synaptic plasticity**

Introduction

AMPA receptors mediate most of the fast EPSC at glutamatergic synapses. AMPA receptors are homotetrameric or heterotetrameric proteins composed of the subunits glutamate receptor 1 (GluR1) to GluR4 (Hollmann and Heinemann, 1994; Rosenmund et al., 1998). Rapid movements of AMPA receptors into and out of the postsynaptic membrane provide a mechanism for the activity-dependent changes in synaptic strength that are thought to underlie aspects of learning and memory (Song and Huganir, 2002).

AMPA receptor trafficking is regulated by numerous AMPA receptor-binding proteins (Song and Huganir, 2002), including the transmembrane protein stargazin (Chen et al., 2000). Absence of stargazin in stargazer mice causes ataxia, seizures, and abnormal head movements (Letts et al., 1998). Cerebellar granule neurons of stargazer mice contain intracellular AMPA receptor protein but essentially lack AMPA receptors on the cell surface, establishing a requirement for stargazin in AMPA receptor trafficking (Hashimoto et al., 1999; Chen et al., 2000). AMPA receptors are unique in their dependence on stargazin for trafficking, because NMDA and kainate receptors occur normally at stargazer granule cell synapses (Chen et al., 2000, 2003). Stargazin belongs to a family of four homologous transmembrane AMPA receptor regulatory proteins (TARPs) with distinct, partially overlapping expression patterns in the brain, and this can explain why the AMPA receptor defect in stargazer mice appears to be restricted to cerebellar granule cells (Tomita et al., 2003).

AMPA receptors from stargazer cerebellum show an immature, endoplasmic reticulum (ER)-type glycosylation pattern, suggesting that stargazin promotes AMPA receptor export from the ER (Tomita et al., 2003). A stringent quality-control system in the ER prevents incompletely folded or assembled proteins from exiting to the Golgi (Ellgaard et al., 1999). Accumulation of unfolded or unassembled proteins in the ER rapidly induces the unfolded protein response, a graded, homeostatic pathway leading to increased transcription of a characteristic set of genes encoding ER chaperones such as Ig binding protein (BiP) (Ma and Hendershot; 2001; Zhang and Kaufman, 2004).

In addition to facilitating AMPA receptor export from the ER (Tomita et al., 2003), stargazin may enhance AMPA receptor surface expression by stabilizing the receptors on the cell membrane. AMPA receptors undergo both constitutive and agonist-induced endocytosis (Carroll et al., 2001). Previous work has shown that stargazin does not prevent agonist-induced endocytosis of AMPA receptors (Tomita et al., 2004). However, whether stargazin affects constitutive AMPA receptor endocytosis has not been explored.

Here, we find that stargazin enhances AMPA receptor surface expression independently of inhibition of constitutive endocytosis. We also show that AMPA receptor expression in TARP-deficient cells, such as heterologous cells or stargazer granule neurons, induces the unfolded protein response (UPR) and that

Received Aug. 30, 2004; revised Dec. 3, 2004; accepted Dec. 13, 2004.

W.V. is supported by a postdoctoral fellowship of the Fund for Scientific Research–Flanders and the Belgian American Educational Foundation. R.A.N. is supported by grants from the National Institutes of Health (NIH) and is a member of the Keck Center for Integrative Neuroscience and the Silvio Conte Center for Neuroscience Research. D.S.B. is supported by grants from the NIH, the Christopher Reeve Paralysis Foundation, and the Human Frontier Science Program, and is an established investigator of the American Heart Association. We thank R. Huganir for GluR1 cDNA, R. Wenthold for GluR6 antibody, K. Mori for p50ATF6 cDNA, R. Austin for BiP cDNA, R. Kelly for dynamin cDNA, L. Jan for $GABA_B$ receptor cDNAs, and A. Wang for technical assistance in the initial stages of this project.

Correspondence should be addressed to Wim Vandenberghe, Department of Neurology, University Hospital Gasthuisberg, Herestraat 49, 3000 Leuven, Belgium. E-mail: wim.vandenberghe@uz.kuleuven.ac.be.

DOI:10.1523/JNEUROSCI.3568-04.2005

this response modulates AMPA receptor surface trafficking. These data support a role for stargazin in regulating AMPA receptor transport through the proximal biosynthetic pathway. Furthermore, our finding that the UPR modulates AMPA receptor trafficking may have important implications for neurological diseases in which the UPR is induced (Ryu et al., 2002; Forman et al., 2003).

Materials and Methods

Plasmid constructs. Rat GluR1 (flip isoform; a kind gift from Dr. R. Huganir, Johns Hopkins University, Baltimore, MD) and GluR6 were tagged with the hemagglutinin (HA) epitope between amino acids 3 and 4 of the mature protein using standard PCR methods. Both constructs were subcloned into the pRK5 vector and verified by sequencing. The stargazin, γ-1, and γ-3 plasmid constructs have been described previously (Chen et al., 2000; Tomita et al., 2003). HA-tagged wild-type and AA/ASRR mutant cDNAs of the $GABA_B$ receptor subunit GB1 (Margeta-Mitrovic et al., 2000) were gifts from Dr. L. Y. Jan [University of California at San Francisco (UCSF)]. A pIRES2 plasmid expressing HA-tagged K44E mutant dynamin I in tandem with enhanced green fluorescent protein (Schmidlin et al., 2001; Dasgupta and Kelly, 2003) was a gift from Dr. R. Kelly (UCSF). BiP cDNA (Werstuck et al., 2001) and p50ATF6 cDNA (Yoshida et al., 2000) were kindly provided by Dr. R. Austin (McMartin University, Hamilton, Canada) and Dr. K. Mori (Kyoto University, Kyoto, Japan), respectively.

Cell cultures and transfection. COS7 cells were cultured as described previously (El-Husseini et al., 2000) and transiently transfected with Lipofectamine Plus (Invitrogen, San Diego, CA). Typically 80 ng of cDNA/cm^2 was transfected. For cotransfections, a 1:2 cDNA ratio of HA–GluR1 and the second construct was used. Transfection efficiencies were usually 30–40% as determined by double staining with the nuclear dye Hoechst 33342 (Molecular Probes, Eugene, OR). All experiments were performed 2 d after transfection.

Dissociated cerebellar granule cell cultures were prepared from 5- to 7-d-old mouse pups (Chen et al., 2000). Stargazer pups were bred from heterozygous parents (The Jackson Laboratory, Bar Harbor, ME). Tail samples were used to genotype pups with the following PCR primers: γ2F, 5′-CATTTCCTGTCTCATCCTTT-3′; γ2R, 5′-ACTGTCACTC-TATCTGGAATC-3′; and γ2KO, 5′-GAGCAAGCAGGTTTCAGGC-3′. Two PCRs were performed on each tail sample: PCR with γ2F and γ2R to amplify the wild-type stargazin allele and PCR with γ2KO and γ2R to detect the knock-out allele. Experiments on granule cell cultures were performed at 4–6 d *in vitro*.

Immunofluorescent assay of surface and intracellular expression. To distinguish surface and intracellular HA-tagged proteins, transfected COS7 cells were washed in PBS and fixed for 30 min in ice-cold 4% paraformaldehyde/PBS. After a subsequent wash in PBS, cells were blocked for 30 min at room temperature (RT) in 5% goat serum/PBS and then incubated for 1 h at RT with monoclonal anti-HA antibody (1:1000; Covance, Berkeley, CA) in 2% goat serum/PBS to allow binding to HA-tagged proteins on the cell surface. After washing in PBS, cells were exposed to cyanine 3-labeled anti-mouse secondary antibody (1:500; Jackson ImmunoResearch, West Grove, PA) in 2% goat serum/PBS for 1 h at RT. Cells were then washed in PBS and permeabilized and blocked for 30 min in 0.1% Triton X-100/5% goat serum/PBS, and incubated for 1 h at RT with anti-HA (1:1000) in 0.1% Triton X-100/2% serum/PBS to allow binding to intracellular HA-tagged protein. After washing in PBS, cells were exposed for 1 h at RT to Alexa Fluor 488 goat anti-mouse secondary antibody (1:10,000; Molecular Probes), washed and mounted in Fluoromount-G (Southern Biotechnology, Birmingham, AL). Images were acquired with a charge-coupled device camera using a 100× oil-immersion objective affixed to an inverted microscope (Axiovert S100TV; Zeiss, Thornwood, NY) and analyzed with MetaMorph software (Universal Imaging Corporation, West Chester, PA).

As a control, the surface/internal staining protocol was applied to COS7 cells transfected with HA-tagged wild-type and AA/ASRR mutant forms of the $GABA_B$ receptor subunit GB1. Wild-type GB1 is completely retained in the ER of transfected COS7 cells, whereas the mutant expresses heavily on the cell surface (Margeta-Mitrovic et al., 2000). Controls consistently showed absence of surface staining in cells transfected with wild-type GB1 (Fig. 1*A*) and strong surface staining after transfection of the mutant (Fig. 1*B*).

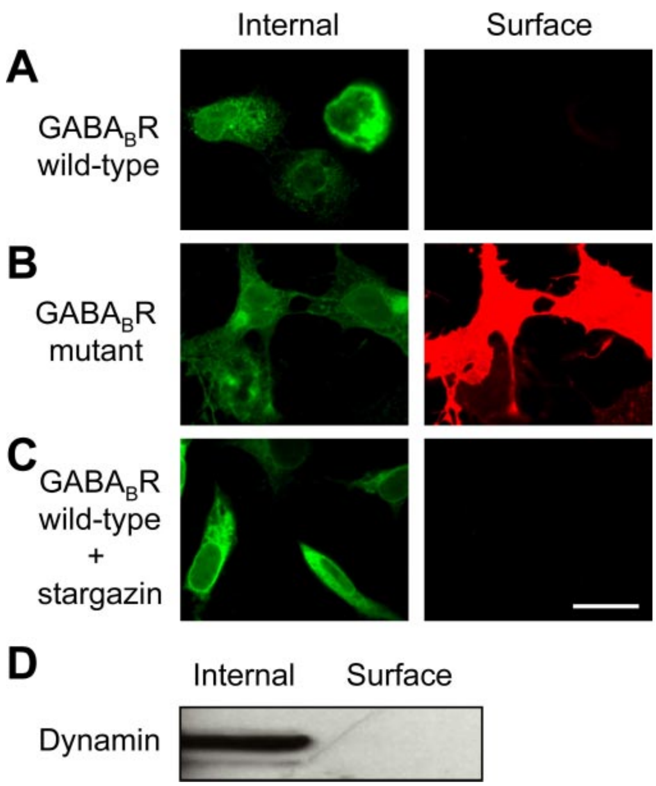

Figure 1. Control experiments for the immunocytochemical and biochemical assays used in this study to distinguish surface and intracellular protein pools. *A–C*, Representative images showing immunostaining with anti-HA before (Surface) and after (Internal) permeabilization with Triton X-100. *A*, COS7 cells were transfected with HA-tagged wild-type $GABA_B$ receptor ($GABA_BR$) GB1 subunit, known to be retained in the ER. *B*, COS7 cells were transfected with the HA-tagged AA/ASRR mutant of the GB1 subunit, known to express heavily on the cell surface. *C*, Wild-type GB1 subunit remains undetectable on the cell surface after coexpression of stargazin. Scale bar, 25 μm. *D*, COS7 cells were transfected with an HA-tagged version of the cytosolic protein dynamin I (K44E mutant) and subjected to the immunoprecipitation assay described in Materials and Methods. After SDS-PAGE of 1% of the internal fraction and 50% of the surface fraction, the blot was probed with anti-dynamin. Dynamin was only detected in the intracellular fraction, excluding contamination of the surface fraction by intracellular protein.

Surface expression of HA-tagged GluR1 or GluR6 relative to intracellular expression was quantified using a strategy similar to that of Okabe et al. (1999) and Standley et al. (2000). All coverslips were coded so that the observer was blinded. Images of internal and surface staining of randomly selected cells were acquired, and the percentage of transfected cells in which surface staining was stronger than intracellular staining was determined. For each condition, at least 30 different fields and 100–200 transfected cells were analyzed (for example, $n = 24$ in Fig. 3*B* refers to a total of 2400–4800 analyzed cells).

For BiP and calnexin staining, cells were fixed, permeabilized, and blocked as described above and incubated with mouse monoclonal anti-KDEL antibody (1:250; Stressgen, Victoria, British Columbia, Canada) or rabbit polyclonal anti-calnexin (1:500; Stressgen), respectively.

Biochemical assay of surface and intracellular expression and Western blotting. Live transfected COS7 cells were washed three times in serum-free medium and incubated for 20 min at 37°C with anti-HA antibody (1:100) in serum-free medium. After three washes in serum-free medium and two washes in ice-cold PBS, cells were resuspended in 200 μl of radioimmunoprecipitation assay (RIPA) buffer (150 mM NaCl, 50 mM Tris, 1% NP-40, 0.5% deoxycholic acid, and 0.1% SDS, pH 8) and solubilized for 30 min at 4°C. Insoluble material was removed by centrifugation at 20,000 × *g* for 4 min. Samples were then incubated with 30 μl of

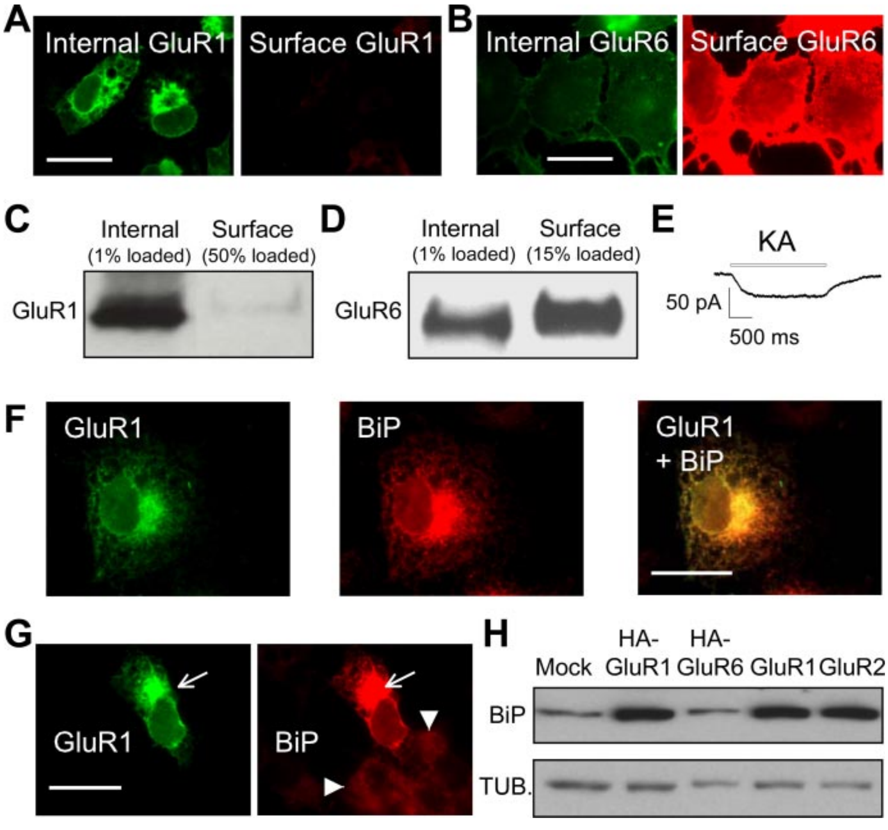

Figure 2. GluR1 expresses poorly on the surface of COS7 cells. *A–D*, COS7 cells were transfected with HA-tagged GluR1 (*A*, *C*) or HA-tagged GluR6 (*B*, *D*). Internal and surface expression was visualized by immunocytochemistry in permeabilized and unpermeabilized conditions, respectively (*A*, *B*), and also measured by Western blotting (*C*, *D*). *E*, In GluR1-transfected cells, detectable currents were induced by 100 μM kainate (KA) at a holding potential of −80 mV. *F–H*, GluR1 colocalizes with the ER chaperone BiP (*F*) and upregulates BiP expression as shown by immunostaining (*G*) and Western blotting (*H*). Arrows and arrowheads in *G* indicate transfected and untransfected cells, respectively. *H*, BiP and tubulin (TUB.) levels were measured in cells transfected with empty vector (Mock) and other constructs as indicated. Scale bars, 25 μm.

protein G (Amersham Biosciences, Arlington Heights, IL) for 45 min at 4°C. Immunoprecipitates were washed five times in ice-cold RIPA buffer. Immunoprecipitates (surface HA-tagged proteins) and supernatants (intracellular HA-tagged proteins) were incubated at 67°C in SDS-PAGE sample buffer for 10 min and then analyzed by SDS-PAGE. Blots were probed with rabbit anti-GluR1 (1:1000; Chemicon, Temecula, CA) or rabbit anti-GluR6 (0.25 μg/ml; a kind gift from Dr. R. J. Wenthold, Laboratory of Neurochemistry, National Institute on Deafness and Other Communication Disorders, Bethesda, MD). Immunoreaction was visualized with the ECL system (Pierce, Rockford, IL). Scanned signals were analyzed with NIH Image software. As a control, COS7 cells were transfected with an HA-tagged version of the cytosolic protein dynamin I (K44E mutant) and subjected to the immunoprecipitation and SDS-PAGE assay described above, followed by immunoblotting with anti-dynamin (H-300; Santa Cruz Biotechnology, Santa Cruz, CA). Dynamin I was exclusively detected in the intracellular fraction (Fig. 1*D*), ruling out contamination of the surface fraction by intracellular protein.

For Western blot analysis of BiP expression, COS7 cells or cerebellar granule cells were solubilized in RIPA buffer as described above, and blots were probed with anti-KDEL antibody (1:250).

Electrophysiology. Whole-cell patch-clamp recordings were performed as described previously (Chen et al., 2000). The extracellular solution contained (in mM): 145 NaCl, 2 $CaCl_2$, 3 KCl, 1.3 $MgSO_4$, 1 NaH_2PO_4, 10 HEPES, and 10 glucose, pH 7.4. The intracellular solution contained (in mM): 140 CsCl, 2 $MgCl_2$, 5 EGTA, 10 HEPES, 0.3 Na_3GTP, and 4 MgATP, pH 7.35. Kainate (Sigma, St. Louis, MO) or *S*-AMPA (Tocris Cookson, Ballwin, MO) were applied locally using solenoid valve-controlled gravity feeding and a perfusion pencil (AutoMate Scientific, San Francisco, CA). Flow through the perfusion pencil was visually confirmed before and after each recording by flow-induced movement of cellular debris near the cell. Current amplitudes were measured using Igor Pro software (WaveMetrics, Lake Oswego, OR).

Statistical analysis. Differences were analyzed using a two-tailed Student's *t* test for comparison between two groups and using ANOVA and a Student–Newman–Keuls test for comparison between more than two groups. Differences were considered significant at $p < 0.05$. Values and error bars in figures denote mean ± SEM.

Results

Stargazin increases AMPA receptor surface expression independently of endocytosis blockade

First we developed a simplified cellular model to study AMPA receptor trafficking by stargazin. We tagged the AMPA receptor subunit GluR1 with an HA epitope in its extracellular N-terminal domain and transfected this construct into COS7 cells, a cell line that lacks AMPA receptors and TARPs. Surface and intracellular GluR1 were visualized by immunocytochemical staining before and after cell permeabilization, respectively. GluR1 expressed poorly on the cell surface (Fig. 2*A*). In contrast, the kainate receptor subunit GluR6, which expressed at similar levels, showed robust surface staining (Fig. 2*B*). We used Western blotting to quantify surface expression of GluR1 and GluR6. Only 0.4 ± 0.1% ($n = 3$) of GluR1 occurred on the cell membrane, compared with 12.5 ± 1.8% ($n = 4$) of GluR6 (Fig. 2*C*,*D*). However, the small surface fraction of GluR1 was functional, because we detected agonist-induced currents (Fig. 2*E*).

Transfected GluR1 showed a perinuclear, reticular distribution and colocalized with the ER chaperones BiP (Fig. 2*F*) and calnexin (data not shown). Interestingly, GluR1-expressing cells showed enhanced BiP staining (Fig. 2*G*). Western blotting confirmed BiP upregulation in cells expressing GluR1 or GluR2, whereas GluR6 had a lesser effect (Fig. 2*H*). Because BiP upregulation is a signature of the UPR (Gething, 1999), this suggested that a large proportion of AMPA receptors was not properly folded or assembled.

Coexpression of stargazin vastly increased the surface expression of GluR1 (Fig. 3*A–D*). In contrast, stargazin had no effect on the distribution of GluR6 (data not shown) or the $GABA_B$ receptor subunit GB1 (Fig. 1*C*), which is retained in the ER of transfected COS7 cells (Margeta-Mitrovic et al., 2000). The effect of stargazin was mimicked by TARP γ-3, the closest stargazin homolog (Tomita et al., 2003), whereas the more distant homolog γ-1 was inactive (Fig. 3*B*,*D*). Consistent with previous studies (Hall et al., 1997), coexpression of GluR2 had no effect on GluR1 surface expression (Fig. 3*B*).

We asked whether stargazin increases surface expression of AMPA receptors by inhibiting endocytosis. In that case, blocking clathrin-mediated endocytosis with a dominant-negative dynamin I mutant (K44E) (Herskovits et al., 1993) should prevent the effect of stargazin. Dominant-negative dynamin increased the surface to internal ratio of GluR1 by ~10-fold (Fig. 4), consistent

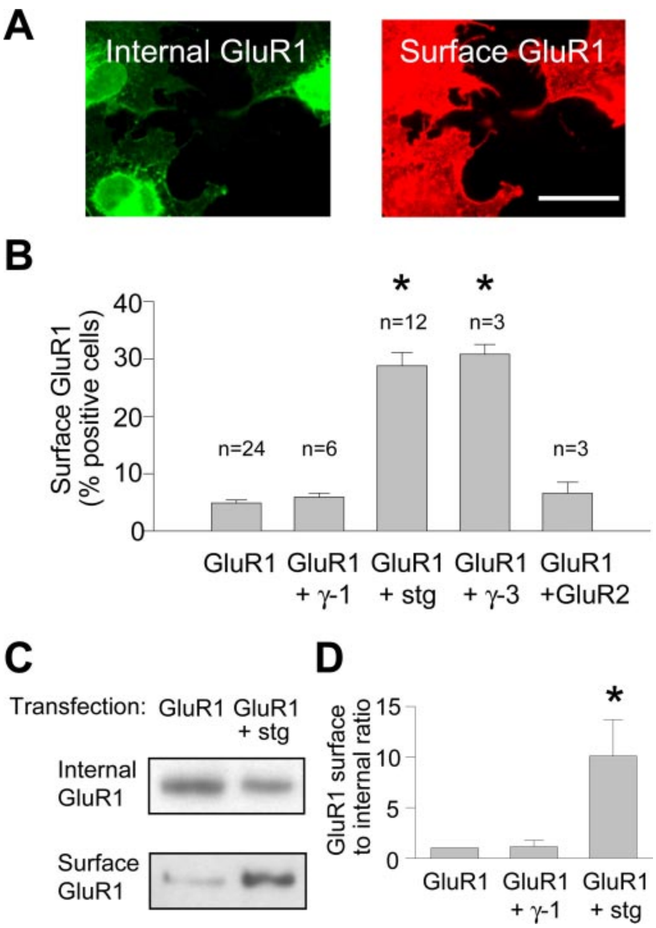

Figure 3. Stargazin promotes surface expression of GluR1 in COS7 cells. *A*, *B*, Cells cotransfected with HA–GluR1 and stargazin (stg) were stained for internal and surface GluR1 (*A*), and the percentage of GluR1-transfected cells showing stronger surface than internal staining was counted (*B*) as described in Materials and Methods. Scale bar, 25 μm. Asterisks in *B* indicate a significant difference ($p < 0.001$ by ANOVA and the Student–Newman–Keuls test) from GluR1 alone. *C*, Western blots showing surface and internal GluR1 expression. Ten percent of the internal fraction and 40% of the surface fraction were loaded. Internal and surface bands were visualized after film exposures of 15 s and 5 min, respectively. *D*, Western blot quantification of GluR1 surface to internal ratios, normalized to the ratio in cells transfected with GluR1 alone ($n = 9$ for each condition). The asterisk indicates a significant difference ($p < 0.001$ by ANOVA and the Student–Newman–Keuls test) from GluR1 plus γ-1.

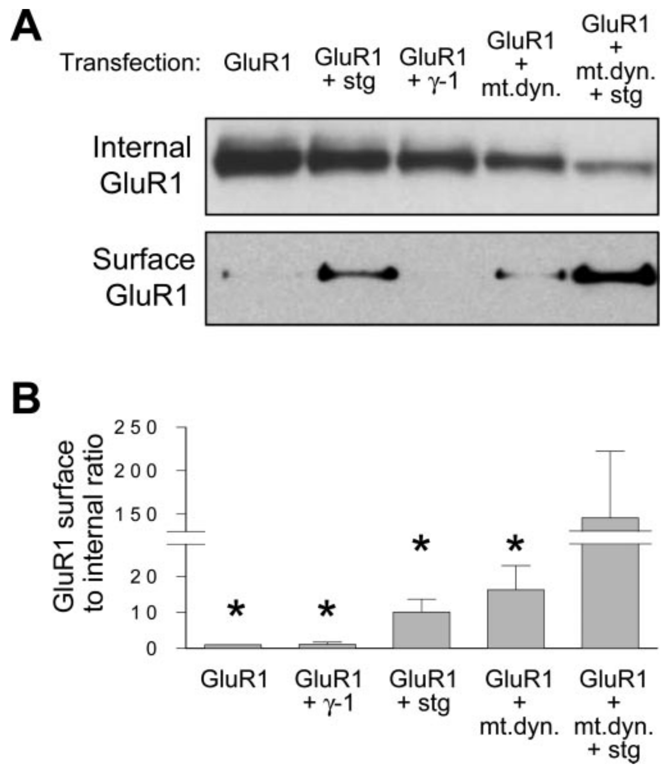

Figure 4. Stargazin functions independently of endocytosis blockade. *A*, COS7 cells were transfected with HA–GluR1, γ-1, stargazin (stg), and dominant-negative dynamin (mt.dyn.). Surface and internal GluR1 were measured using Western blotting after loading 10% of the internal fraction and 40% of the surface fraction. Internal and surface bands were visualized after film exposures of 15 s and 5 min, respectively. *B*, Quantification of GluR1 surface to internal ratios, normalized to the ratio in cells transfected with GluR1 alone ($n = 5$–8). Asterisks indicate a significant difference ($p < 0.01$ by ANOVA and the Student–Newman–Keuls test) from GluR1 plus mt.dyn. plus stg.

with previous reports of constitutive GluR1 endocytosis (Man et al., 2000). However, stargazin and dominant-negative dynamin synergized to increase the surface fraction of AMPA receptors by ~100-fold (Fig. 4). This synergistic effect indicated that stargazin does not function by inhibiting AMPA receptor endocytosis.

The UPR mimics the effect of stargazin

The BiP upregulation induced by GluR1 transfection (Fig. 2*G,H*) suggested that GluR1 folding or assembly was inefficient. In this case, additional upregulation of ER chaperones by stronger UPR induction might promote surface expression of GluR1. Drugs such as tunicamycin, thapsigargin, or dithiothreitol induce the UPR by disrupting ER protein folding (Zhang and Kaufman, 2004) and, not surprisingly, all reduced GluR1 surface expression to undetectable levels (data not shown). In contrast, proteasome inhibitors strongly induce the UPR without interfering with protein folding (Bush et al., 1997; Sitia and Braakman, 2003; Zhang and Kaufman, 2004). Therefore, we treated GluR1-transfected cells with the structurally unrelated proteasome inhibitors lactacystin and carbobenzoxy-L-leucyl-L-leucyl-L-leucinal (MG-132). Both proteasome inhibitors increased BiP protein levels within 6 h (data not shown), and they greatly increased the surface fraction of GluR1 (Fig. 5*A–C*) but not the $GABA_B$ receptor subunit GB1 (data not shown). In contrast, the lysosomal inhibitor E64-d, which does not induce the UPR, had no effect on GluR1 distribution (Fig. 5*G*). The effects of proteasome inhibitors were dose and time dependent (Fig. 5*D,E*) and did not reflect changes in the total amount of GluR1, because these levels were not increased by up to 10 h of treatment with proteasome inhibitors (Fig. 5*F*).

If transcriptional upregulation of UPR effector proteins mediates the effect of proteasome inhibitors on GluR1 distribution, protein synthesis inhibitors should block this effect. Indeed, the protein synthesis inhibitor cycloheximide completely abolished the effect of MG-132 on GluR1 distribution (Fig. 5*G*). Furthermore, genistein, a tyrosine kinase inhibitor that prevents full expression of the UPR through inactivation of the transcription factor nuclear factor Y (NF-Y) (also known as CCAAT binding factor) (Cao et al., 1995; Zhou and Lee, 1998; Nyfeler et al., 2003), significantly reduced the effect of MG-132 on GluR1 surface trafficking (Fig. 5*G*).

We also upregulated the unfolded protein response using a constitutively active form of the transcription factor ATF6 (activating transcription factor 6) (p50ATF6) (Haze et al., 1999). Activation of ATF6 occurs exclusively in the context of the UPR and induces transcription of ER chaperones (Haze et al., 1999; Ma and Hendershot, 2001; Zhang and Kaufman, 2004). Transfection of constitutively active ATF6 increased the levels of ER chaper-

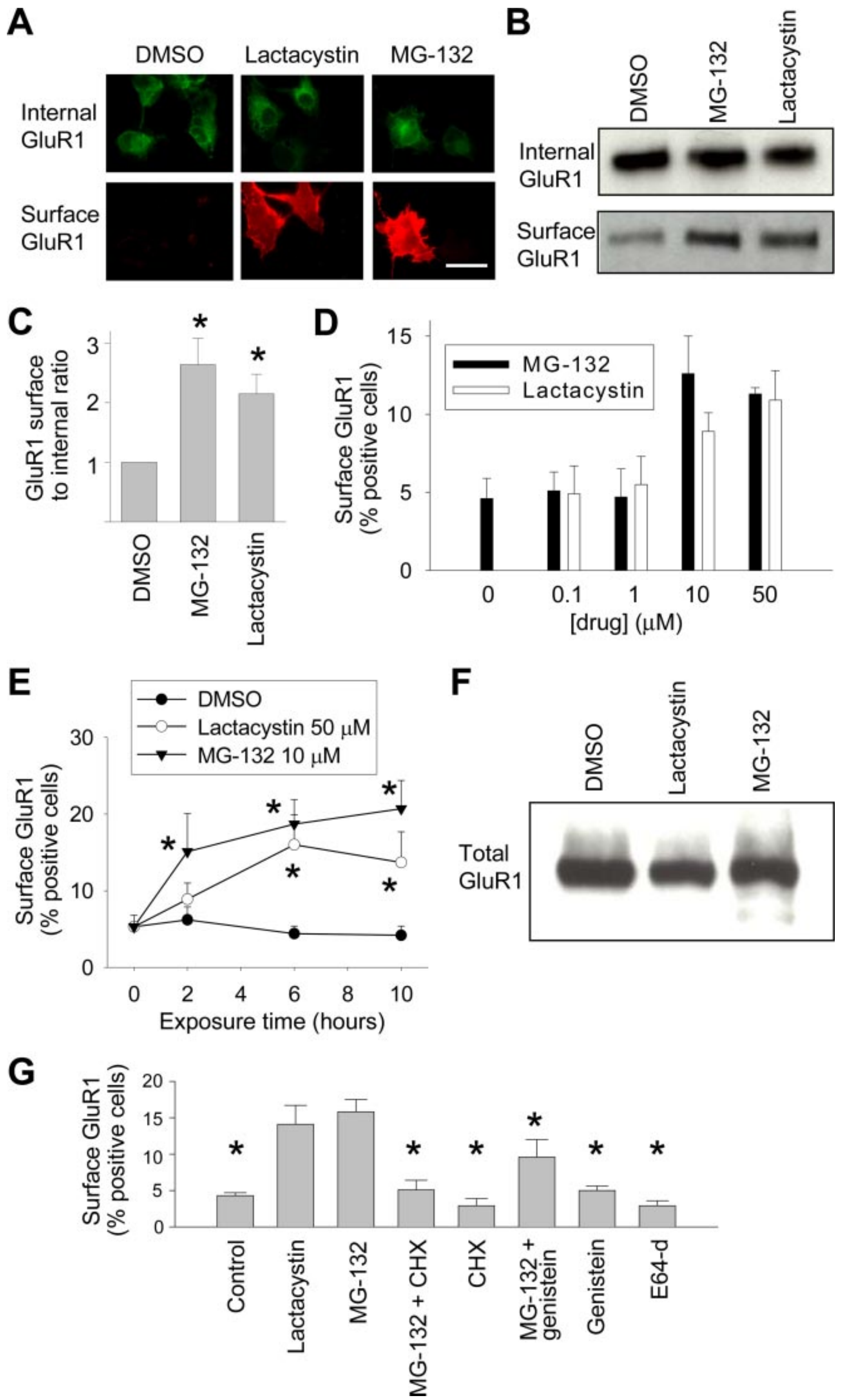

Figure 5. UPR induction by proteasome inhibitors promotes GluR1 surface trafficking. *A*, COS7 cells were treated for 10 h with the proteasome inhibitors lactacystin (10 μM) or MG-132 (10 μM) or with a DMSO control and then stained for internal and surface GluR1. Scale bar, 25 μm. *B*, Western blots showing internal and surface GluR1 expression in COS7 cells treated for 6 h with MG-132 (10 μM), lactacystin (50 μM), or DMSO. Ten percent of the internal fraction and 40% of the surface fraction were loaded. Internal and surface bands were visualized after film exposures of 15 s and 5 min, respectively. *C*, Western blot quantification of GluR1 surface to internal ratios, normalized to the ratio in cells treated with DMSO control ($n = 4$ for each condition). COS7 cells were treated with MG-132 (10 μM), lactacystin (50 μM), or DMSO for 6 h. Asterisks indicate a significant difference ($p < 0.05$ by ANOVA and the Student–Newman–Keuls test) from the DMSO control. *D*, Dose dependence of the effect of proteasome inhibitors (6 h) on GluR1 distribution ($n = 3$). *E*, Time course of the effect of proteasome inhibition on immunocytochemical GluR1 distribution ($n = 5$ for each time point). Asterisks indicate a significant difference ($p < 0.01$ by ANOVA and the Student–Newman–Keuls test) from the DMSO control at the same time point. *F*, Western blot of total GluR1 levels after treatment for 10 h with lactacystin (10 μM), MG-132 (10 μM), or the DMSO control. *G*, COS7 cells were stained for internal and surface GluR1 after treatment with 50 μM lactacystin for 6 h, 10 μM MG-132 for 6 h, 50 μg/ml cycloheximide (CHX) for 7 h, 140 μM genistein for 7 h, or 10 μM E64-d for 12 h. Cycloheximide or genistein was added 1 h before treatment with MG-132. Asterisks indicate a significant difference ($p < 0.05$ by ANOVA and the Student–Newman–Keuls test) from MG-132 ($n =$ at least 3 for each condition).

ones such as BiP (Fig. 6*A*), and significantly enhanced the surface fraction of GluR1 (Fig. 6*B,C*). In contrast, BiP overexpression alone had no effect (data not shown), suggesting that the concerted UPR is required for GluR1 redistribution.

Proteasome inhibitors had no significant effect on GluR1 distribution in cells transfected with stargazin, as measured immunocytochemically (Fig. 7*A*). Immunoprecipitation experiments confirmed that the effects of stargazin and proteasome inhibitors were not additive: stargazin alone increased the surface fraction of GluR1 by a factor of 8.0 ± 2.3, whereas stargazin combined with MG-132 (10 μM, 6 h) or stargazin combined with lactacystin (50 μM, 6 h) increased this fraction by a factor of 7.0 ± 3.6 or 9.3 ± 3.0, respectively ($n = 4$; no significant difference between the three conditions, $p = 0.8$ by ANOVA). Similarly, expression of p50ATF6 did not increase GluR1 surface expression in cells transfected with stargazin (data not shown). These results suggested that stargazin and the UPR have a shared mechanism of action. Furthermore, BiP levels were similar in cells transfected with stargazin or γ-1 alone, indicating that induction of the UPR did not account for the effect of stargazin on GluR1 (Fig. 7*B*). Finally, UPR inhibition with genistein did not reduce the effect of stargazin (data not shown). These experiments suggested a direct, chaperone-like effect of stargazin on folding or assembly of the AMPA receptor complex.

The UPR is induced in cerebellar granule neurons from stargazer mice

To explore these mechanisms in neurons, we took advantage of stargazer mice, which lack TARP function in cerebellar granule neurons (Chen et al., 2000). As reported previously, AMPA receptor currents in stargazer granule neurons were <10% of those in wild-type neurons (Fig. 8*C,D*) (Hashimoto et al., 1999; Chen et al., 2000). Interestingly, we detected increased BiP levels in stargazer granule cell cultures (Fig. 8*A,B*), suggesting that a compensatory UPR induction helps fold or assemble AMPA receptors. Consistent with this, the residual currents in stargazer neurons were reduced by suppressing the UPR with genistein (Fig. 8*C,D*). In contrast, genistein treatment did not diminish currents in wild-type neurons (Fig. 8*C,D*).

Discussion

Stargazin promotes AMPA receptor traffic through the early biosynthetic pathway

The present study provides several new insights into the cellular mechanism for the

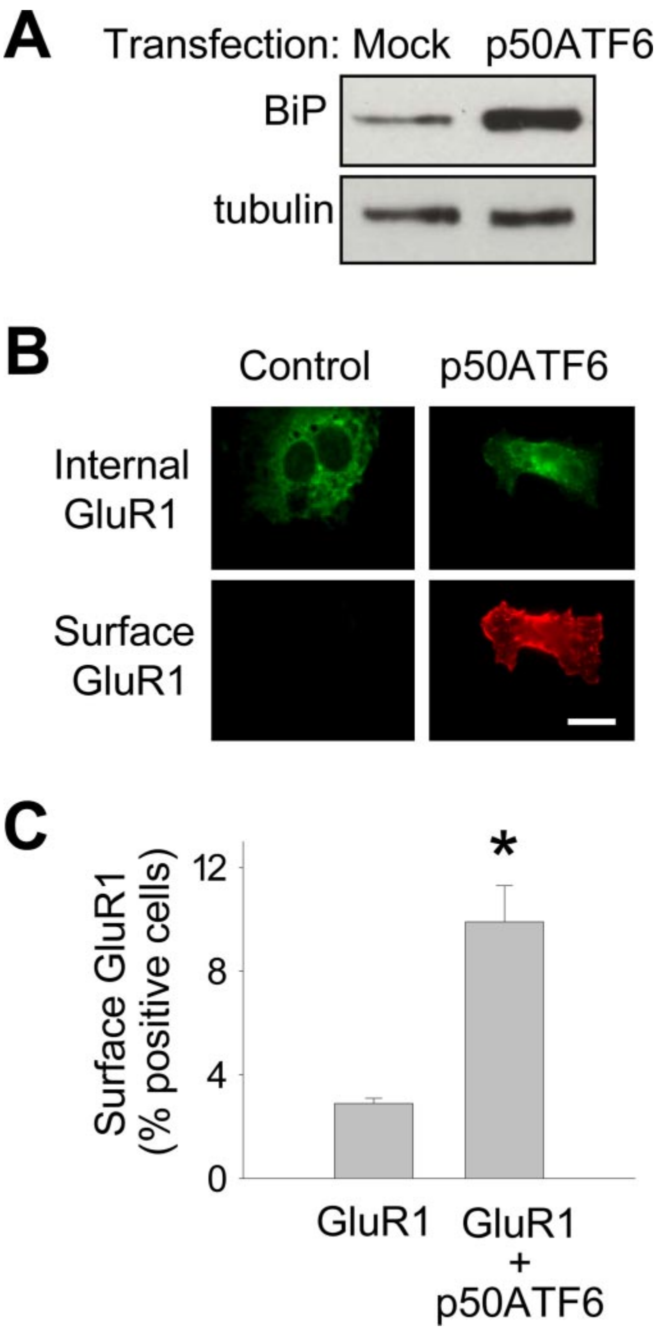

Figure 6. UPR induction by ATF6 promotes GluR1 surface expression. *A*, Western blotting shows BiP upregulation by activated ATF6 (p50ATF6). *B*, COS7 cells cotransfected with HA–GluR1 alone (control) or HA–GluR1 and p50ATF6 were stained for internal and surface GluR1. Scale bar, 25 μm. *C*, Quantification of the effect of p50ATF6 on GluR1 distribution ($n = 3$). The asterisk indicates significant difference ($p < 0.01$ by two-tailed Student's *t* test) from GluR1.

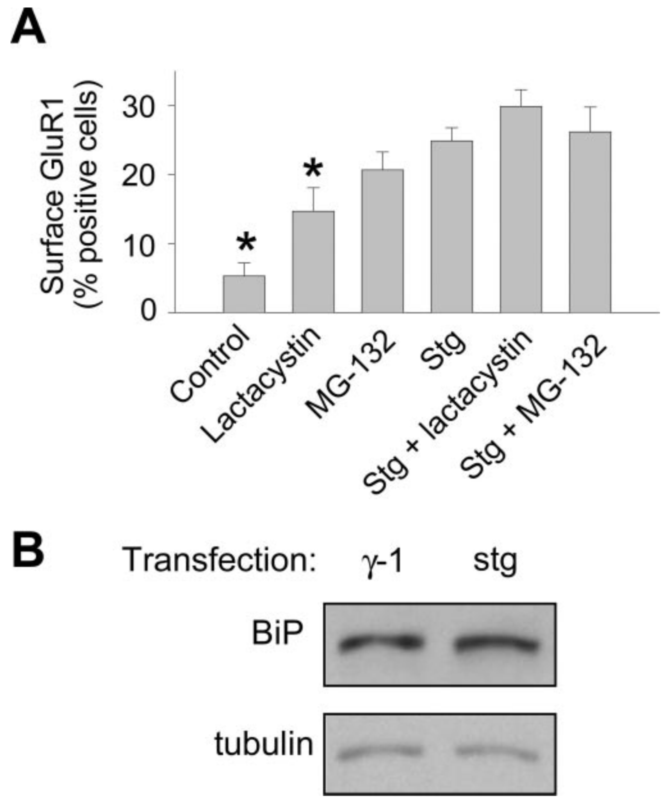

Figure 7. Stargazin occludes the effect of UPR induction on GluR1 surface trafficking. *A*, COS7 cells were transfected with HA–GluR1 in the absence or presence of stargazin (Stg); treated for 10 h with lactacystin (50 μM), MG-132 (10 μM), or DMSO; and stained for surface and internal GluR1 ($n = 3$–7). Asterisks indicate a significant difference ($p < 0.05$ by ANOVA and the Student–Newman–Keuls test) from stargazin. *B*, Western blot showing similar BiP levels in COS7 cells transfected with γ-1 or stargazin (stg).

effect of stargazin on AMPA receptor surface expression. First, this mechanism does not involve inhibition of constitutive AMPA receptor endocytosis. Second, the UPR is induced in cerebellar granule neurons from stargazer mice. Because the UPR is triggered exclusively by increased amounts of unfolded or unassembled proteins in the ER (Casagrande et al., 2000; Ma and Hendershot, 2001; Zhang and Kaufman, 2004), this implies a role for stargazin in AMPA receptor folding or assembly. This role for stargazin in AMPA receptor transport through the early compartments of the biosynthetic pathway is consistent with the immature glycosylation of AMPA receptors in stargazer cerebellum (Tomita et al., 2003).

In addition to being upregulated by the UPR, the ER chaperone BiP serves as the central regulator for UPR induction (Gething, 1999; Zhang and Kaufman, 2004). BiP transiently binds to newly synthesized polypeptides and more permanently to misfolded or misassembled proteins. The immediate trigger for UPR induction is the decrease in free BiP concentration that occurs when BiP is sequestered into complexes with unfolded or unassembled proteins. Interestingly, BiP and AMPA receptors coimmunoprecipitate from brain extracts (Rubio and Wenthold, 1999), providing a direct link between accumulation of unfolded or unassembled AMPA receptors and UPR induction.

The role of stargazin in AMPA receptor trafficking is reminiscent of that of client-specific escort chaperones such as ninaA, which accompany their substrates out of the ER (Colley et al., 1991; Ellgaard et al., 1999; Herrmann et al., 1999). However, stargazin is not a chaperone in the strictest sense, because traditional chaperones bind their substrates only transiently (Ellgaard et al., 1999; Agashe and Hartl, 2000). In contrast, the association of TARPs with surface AMPA receptors (Tomita et al., 2004) suggests that stargazin is part of the final, functional AMPA receptor complex. Future studies will be required to define the detailed molecular mechanism for the forward-trafficking effect of stargazin.

Proteins that persist in an incompletely folded or assembled state are often retrotranslocated into the cytosol and eliminated by ER-associated degradation (ERAD) (Tsai et al., 2002). Simi-

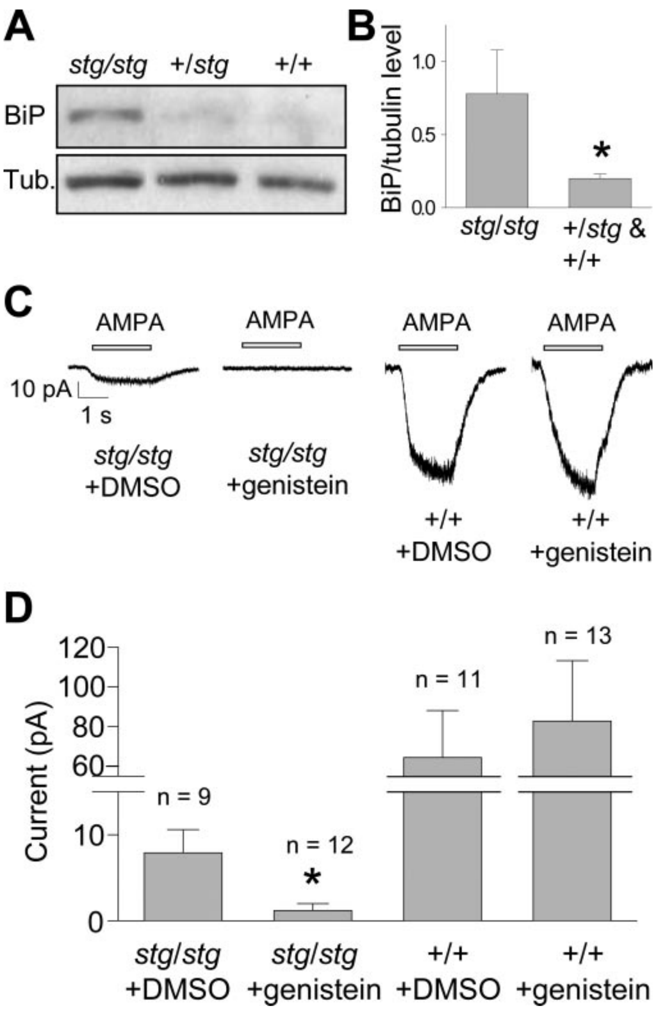

Figure 8. The UPR induced in stargazer neurons traffics residual functional AMPA receptors. *A*, Western blots showing BiP and tubulin (Tub.) levels in cerebellar granule cell cultures from stargazer (*stg/stg*), heterozygous (+/*stg*), and wild-type (+/+) littermates. *B*, BiP protein levels in cerebellar granule cell cultures from nine stargazer pups and 23 heterozygous and wild-type littermates. The asterisk indicates a significant difference ($p = 0.01$ by two-tailed Student's *t* test) from stargazer. *C, D*, Whole-cell currents induced by 10 μM AMPA in cultured cerebellar granule neurons from stargazer mice (*stg/stg*) are ~10% of those from wild-type (+/+) littermates. Genistein (140 μM, 20 h) selectively suppresses residual AMPA-induced currents in stargazer neurons. The asterisk in *D* indicates a significant difference ($p = 0.01$ by two-tailed Student's *t* test) from DMSO treatment.

larly, AMPA receptors that persistently fail to associate with stargazin may eventually be degraded. This would explain the selective reduction of total AMPA receptor protein levels in stargazer cerebellum (Tomita et al., 2003). That AMPA receptors can be ERAD substrates *in vivo* is plausible based on the observation of ubiquitinated, AMPA receptor-immunoreactive inclusions in the cytosol of a population of spinal interneurons (Serrando et al., 2002).

The present findings in COS7 cells and stargazer granule neurons and previous studies in oocytes (Chen et al., 2003) indicate that a very small fraction of AMPA receptors reaches the cell surface in the absence of stargazin. Our data show that induction of the UPR contributes to this inefficient AMPA receptor trafficking pathway. Apparently, some UPR targets may help convert AMPA receptors into an ER export-competent state or may relax retention mechanisms. This is consistent with a recent report showing a specific role for the UPR in ER export of glutamate receptors in *Caenorhabditis elegans*, an organism that lacks close homologs of stargazin (Shim et al., 2004).

What could be the physiological purpose of TARP-dependent AMPA receptor trafficking? One possibility would be to guarantee clustering of AMPA receptors at postsynaptic sites. TARPs contain a C-terminal postsynaptic density-95/Discs large/zona occludens-1 (PDZ)-binding domain, and this domain is necessary for synaptic targeting of AMPA receptors (Chen et al., 2000). The forward-trafficking function of TARPs may thus ensure that surface AMPA receptors associate with PDZ proteins, thereby tethering them to the synapse and reducing extrasynaptic expression.

Potential implications for neurological diseases

The present study provides the first evidence that the UPR can enhance AMPA receptor surface trafficking in vertebrate cells. This may have important implications for the pathogenesis of neurological diseases in which the UPR is induced (Forman et al., 2003). For example, the UPR is activated in cellular models of Parkinson's disease (Ryu et al., 2002; Holtz and O'Malley, 2003) and in brains of Parkinson's disease patients with parkin mutations (Imai et al., 2001). Convincing evidence for UPR induction is also found in Pelizaeus–Merzbacher disease, a leukodystrophy caused by mutations in the *proteolipid protein* gene leading to apoptosis of oligodendrocytes (Southwood et al., 2002). Enhanced AMPA receptor surface trafficking attributable to UPR activation may increase cellular susceptibility to excitotoxicity and thus accelerate death of dopaminergic neurons or oligodendrocytes (Beal, 1998; Matute et al., 2001).

References

Agashe VR, Hartl FU (2000) Roles of molecular chaperones in cytoplasmic protein folding. Semin Cell Dev Biol 11:15–25.

Beal MF (1998) Excitotoxicity and nitric oxide in Parkinson's disease pathogenesis. Ann Neurol 44:S110–S114.

Bush KT, Goldberg AL, Nigam SK (1997) Proteasome inhibition leads to a heat-shock response, induction of endoplasmic reticulum chaperones, and thermotolerance. J Biol Chem 272:9086–9092.

Cao X, Zhou Y, Lee AS (1995) Requirement of tyrosine and serine/threonine kinases in the transcriptional activation of the mammalian grp78/BiP promoter by thapsigargin. J Biol Chem 270:494–502.

Carroll RC, Beattie EC, von Zastrow M, Malenka RC (2001) Role of AMPA receptor endocytosis in synaptic plasticity. Nat Rev Neurosci 2:315–324.

Casagrande R, Stern P, Diehn M, Shamu C, Osario M, Zuniga M, Brown PO, Ploegh H (2000) Degradation of proteins from the ER of *S. cerevisiae* requires an intact unfolded protein response pathway. Mol Cell 5:729–735.

Chen L, Chetkovich DM, Petralia RS, Sweeney NT, Kawasaki Y, Wenthold RJ, Bredt DS, Nicoll RA (2000) Stargazin regulates synaptic targeting of AMPA receptors by two distinct mechanisms. Nature 408:936–943.

Chen L, El-Husseini A, Tomita S, Bredt DS, Nicoll RA (2003) Stargazin differentially controls the trafficking of α-amino-3-hydroxyl-5-methyl-4-isoxazolepropionate and kainate receptors. Mol Pharmacol 64:703–706.

Colley NJ, Baker EK, Stamnes MA, Zuker CS (1991) The cyclophilin homolog ninaA is required in the secretory pathway. Cell 67:255–263.

Dasgupta S, Kelly RB (2003) Internalization signals in synaptotagmin VII utilizing two independent pathways are masked by intramolecular inhibitions. J Cell Sci 116:1327–1337.

El-Husseini AE, Topinka JR, Lehrer-Graiwer JE, Firestein BL, Craven SE, Aoki C, Bredt DS (2000) Ion channel clustering by membrane-associated guanylate kinases. Differential regulation by N-terminal lipid and metal binding motifs. J Biol Chem 275:23904–23910.

Ellgaard L, Molinari M, Helenius A (1999) Setting the standards: quality control in the secretory pathway. Science 286:1882–1888.

Forman MS, Lee VM, Trojanowski JQ (2003) "Unfolding" pathways in neurodegenerative disease. Trends Neurosci 26:407–410.

Gething MJ (1999) Role and regulation of the ER chaperone BiP. Semin Cell Dev Biol 10:465–472.

Hall RA, Hansen A, Andersen PH, Soderling TR (1997) Surface expression of the AMPA receptor subunits GluR1, GluR2, and GluR4 in stably transfected baby hamster kidney cells. J Neurochem 68:625–630.

Hashimoto K, Fukaya M, Qiao X, Sakimura K, Watanabe M, Kano M (1999) Impairment of AMPA receptor function in cerebellar granule cells of ataxic mutant mouse stargazer. J Neurosci 19:6027–6036.

Haze K, Yoshida H, Yanagi H, Yura T, Mori K (1999) Mammalian transcription factor ATF6 is synthesized as a transmembrane protein and activated by proteolysis in response to endoplasmic reticulum stress. Mol Biol Cell 10:3787–3799.

Herrmann JM, Malkus P, Schekman R (1999) Out of the ER–outfitters, escorts and guides. Trends Cell Biol 9:5–7.

Herskovits JS, Burgess CC, Obar RA, Vallee RB (1993) Effects of mutant rat dynamin on endocytosis. J Cell Biol 122:565–578.

Hollmann M, Heinemann S (1994) Cloned glutamate receptors. Annu Rev Neurosci 17:31–108.

Holtz WA, O'Malley KL (2003) Parkinsonian mimetics induce aspects of unfolded protein response in death of dopaminergic neurons. J Biol Chem 278:19367–19377.

Imai Y, Soda M, Inoue H, Hattori N, Mizuno Y, Takahashi R (2001) An unfolded putative transmembrane polypeptide, which can lead to endoplasmic reticulum stress, is a substrate of parkin. Cell 105:891–902.

Letts VA, Felix R, Biddlecome GH, Arikkath J, Mahaffey CL, Valenzuela A, Bartlett II FS, Mori Y, Campbell KP, Frankel WN (1998) The mouse stargazer gene encodes a neuronal Ca^{2+}-channel gamma subunit. Nat Genet 19:340–347.

Ma Y, Hendershot LM (2001) The unfolding tale of the unfolded protein response. Cell 107:827–830.

Man HY, Lin JW, Ju WH, Ahmadian G, Liu L, Becker LE, Sheng M, Wang YT (2000) Regulation of AMPA receptor-mediated synaptic transmission by clathrin-dependent receptor internalization. Neuron 25:649–662.

Margeta-Mitrovic M, Jan YN, Jan LY (2000) A trafficking checkpoint controls GABA(B) receptor heterodimerization. Neuron 27:97–106.

Matute C, Alberdi E, Domercq M, Perez-Cerda F, Perez-Samartin A, Sanchez-Gomez MV (2001) The link between excitotoxic oligodendroglial death and demyelinating diseases. Trends Neurosci 24:224–230.

Nyfeler B, Nufer O, Matsui T, Mori K, Hauri HP (2003) The cargo receptor ERGIC-53 is a target of the unfolded protein response. Biochem Biophys Res Commun 304:599–604.

Okabe S, Miwa A, Okado H (1999) Alternative splicing of the C-terminal domain regulates cell surface expression of the NMDA receptor NR1 subunit. J Neurosci 19:7781–7792.

Rosenmund C, Stern-Bach Y, Stevens CF (1998) The tetrameric structure of a glutamate receptor channel. Science 280:1596–1599.

Rubio ME, Wenthold RJ (1999) Calnexin and the immunoglobulin binding protein (BiP) coimmunoprecipitate with AMPA receptors. J Neurochem 73:942–948.

Ryu EJ, Harding HP, Angelastro JM, Vitolo OV, Ron D, Greene LA (2002) Endoplasmic reticulum stress and the unfolded protein response in cellular models of Parkinson's disease. J Neurosci 22:10690–10698.

Schmidlin F, Dery O, DeFea KO, Slice L, Patierno S, Sternini C, Grady EF, Bunnett NW (2001) Dynamin and Rab5a-dependent trafficking and signaling of the neurokinin 1 receptor. J Biol Chem 276:25427–25437.

Serrando M, Casanovas A, Esquerda JE (2002) Occurrence of glutamate receptor subunit 1-containing aggresome-like structures during normal development of rat spinal cord interneurons. J Comp Neurol 442:23–34.

Shim J, Umemura T, Nothstein E, Rongo C (2004) The unfolded protein response regulates glutamate receptor export from the endoplasmic reticulum. Mol Biol Cell 15:4818–4828.

Sitia R, Braakman I (2003) Quality control in the endoplasmic reticulum protein factory. Nature 426:891–894.

Song I, Huganir RL (2002) Regulation of AMPA receptors during synaptic plasticity. Trends Neurosci 25:578–588.

Southwood CM, Garbern J, Jiang W, Gow A (2002) The unfolded protein response modulates disease severity in Pelizaeus–Merzbacher disease. Neuron 36:585–596.

Standley S, Roche KW, McCallum J, Sans N, Wenthold RJ (2000) PDZ domain suppression of an ER retention signal in NMDA receptor NR1 splice variants. Neuron 28:887–898.

Tomita S, Chen L, Kawasaki Y, Petralia RS, Wenthold RJ, Nicoll RA, Bredt DS (2003) Functional studies and distribution define a family of transmembrane AMPA receptor regulatory proteins. J Cell Biol 161:805–816.

Tomita S, Fukata M, Nicoll RA, Bredt DS (2004) Dynamic interaction of stargazin-like TARPs with cycling AMPA receptors at synapses. Science 303:1508–1511.

Tsai B, Ye Y, Rapoport TA (2002) Retro-translocation of proteins from the endoplasmic reticulum into the cytosol. Nat Rev Mol Cell Biol 3:246–255.

Werstuck GH, Lentz SR, Dayal S, Hossain GS, Sood SK, Shi YY, Zhou J, Maeda N, Krisans SK, Malinow MR, Austin RC (2001) Homocysteine-induced endoplasmic reticulum stress causes dysregulation of the cholesterol and triglyceride biosynthetic pathways. J Clin Invest 107:1263–1273.

Yoshida H, Okada T, Haze K, Yanagi H, Yura T, Negishi M, Mori K (2000) ATF6 activated by proteolysis binds in the presence of NF-Y (CBF) directly to the cis-acting element responsible for the mammalian unfolded protein response. Mol Cell Biol 20:6755–6767.

Zhang K, Kaufman RJ (2004) Signaling the unfolded protein response from the endoplasmic reticulum. J Biol Chem 279:25935–25938.

Zhou Y, Lee AS (1998) Mechanism for the suppression of the mammalian stress response by genistein, an anticancer phytoestrogen from soy. J Natl Cancer Inst 90:381–388.